Rev.Adv.Mater.Sci. 18(2008) 56-60

ANALYSIS OF COMPOSITION DEPENDENCE OF FORMATION OF TERNARY BULK METALLIC GLASSES FROM CRYSTALLOGRAPHIC DATA ON TERNARY COMPOUNDS

A. Takeuchi[1], S. Ranganathan[2], B.S. Murty[3] and A. Inoue[1]

[1]Institute for Materials Research, Tohoku University, Sendai 980 8577, Japan
[2]Department of Metallurgy, Indian Institute of Science, Bangalore 560 012, India
[3]Department of Metallurgical and Materials Engineering, Indian Institute of Technology, Madras, Chennai 600 036, India

Received: March 29, 2008

Abstract. The composition dependence of formation of ternary bulk metallic glasses (BMGs) has been analyzed with crystallographic data concerning 16873 ternary compounds with a composition triangle named L-M-S diagram for relative atomic size of constituent elements of L (Large), M (interMediate), and S (Small). As well as ternary compounds containing Cu_2Mg, Fe_2P and C_6Cr_{23} types, three types of ternary BMGs characterized by the relative atomic size of the main element of L- (La-, Zr-, Pd- and Ca-based BMGs), M- (Fe- and Mg-based BMGs) and S-types (Cu-based BMGs) are plotted in the L-M-S diagram. The L-M-S diagram with plots of all ternary compounds reveals a general tendency that the ternary compounds are frequently formed in the S-rich corner as compared to L- and M-rich corners. The L-M-S diagram shows that Fe_2P and C_6Cr_{23} type compounds directly affect the formation of M-type BMGs and also possibly influence the formation of the L-type BMGs. The high glass-forming ability of La-, Zr- and Ca-based BMGs is due to features of their composition regions in the L-M-S diagram wherein ternary compounds infrequently appear and anti-Laves relationship to Cu_2Mg type compounds holds in ternary systems.

1. INTRODUCTION

Recently, unprecedented interest has been paid to metallic glasses in the field of materials science and engineering since the first success in their fabrication in 1960 [1]. In part, this is due to the success in fabricating a number of multicomponent metallic glasses into bulk shape, known as bulk metallic glasses (BMGs) [2]. Several studies have been conducted to explain the formability of glassy phase with respect to stoichiometry of binary compounds. For instance, the earliest research made by Hume-Rothery and Anderson [3] clarifies that the approximate atomic ratios of 1:6, 1:3, 1:2, and 2.3 are favorable for eutectic compositions and that quasi-stoichiometric compositions of $A_{12}B$ can be stable as a liquid phase from considerations with the Frank icosahedral unit. On the other hand, Chen [4] pointed out some of the stable compounds of A_3B and A_2B types affecting the stability of glassy phase. Furthermore, Amand and Giessen [5] reported the important stoichiometry of A_2B in Ca-based binary metallic glasses, which were termed as anti-Laves composition.

These reported results from stoichiometric, geometrical and structural points of view give important insights into the stabilization mechanism of the glassy phase. However, general remarks have not been established yet for multicomponent

Corresponding author: A. Takeuchi, e-mail: takeuchi@imr.tohoku.ac.jp

Table 1. Ten structure types that frequently appear in the ternary phase diagrams and the numbers of compounds (Nos. compounds) [16]. The coordination symbol (CS), coordination number (CN) and coordination notation of each structure type is from Pettifor map [15]. The total numbers of ternary compounds are amounted to be 16873 [16], and the ten structure types account for approximately 20% of all the ternary compounds.

No.	Structure type	Nos. compounds	CS	CN	Coordination notation
1	Al_4Ba	624	bc	4/5	$4^{3.0}/4^{2.1}1^{4.0}$
2	Cu_2Mg	474	ry3	12/16	$12^{5.0}/12^{5.0}4^{6.0}$
3	ClNa	392	d4	6	$6^{4.0}$
4	Co_2Si	371	ms	10/13	$8^{5.0}2^{4.0}/10^{5.0}2^{6.0}1^{4.0}$
5	Fe_2P	336	kr	9/12	$6^{5.0}3^{4.0}/12^{5.0}$
6	$MgZn_2$	330	ry	12/16	$12^{5.0}/12^{5.0}4^{6.0}$
7	BiF_3	296	w5	14	$8^{0.3}6^{0.4}$
8	$Mn_{12}Th$	231	rv1	12/14	$12^{5.0}/12^{5.0}2^{6.0}$
9	P_4Th_3	219	df	6/8	$6^{4.0}/4^{5.0}4^{4.0}$
10	$CaCu_5$	212	qr	12/12	$12^{2.2}$(h)$/12^{5.0}$

alloy systems containing more than two elements, except for the results reported by Miracle [11]. The aim of the present study is to clarify the general trends of the composition dependence of formation of ternary BMGs from the crystallographic data on ternary compounds in terms of their stoichiometry and local atomic arrangements of their structure in a scheme to pay attention to the atomic order similar to that in competing crystalline structures.

2. METHODS

The ternary BMGs and compounds are plotted in a composition triangle termed as L-M-S composition diagram, wherein the elements at the corners are determined by their relative atomic size of constituent elements in the order of L (Large), M (interMediate), and S (Small). In case of constituent elements with the same atomic radius, the element with greater atomic number is to be the larger atomic radius. The values of atomic radius of elements are quoted from our previous study [12], in which the data are quoted from the original literatures [13,14].

The crystallographic data on binary systems including their local atomic arrangements are quoted from Pettifor map [15] as supplemental data, and those on ternary systems are from ternary phase diagrams [16]. Table 1 shows ten structure types that frequently appear in the ternary phase diagrams and the numbers of the ternary compounds [16], together with the coordination symbol (CS), coordination number (CN) and coordination notation from Pettifor map [15]. Among a number of ternary compounds, we focused on the ternary compounds with structure types of Cu_2Mg, Fe_2P and C_6Cr_{23} according to the following aspects. Firstly, Cu_2Mg and Fe_2P types are the second and the fifth major ternary compounds and the C_6Cr_{23} [10] type is widely accepted as a structural unit for the local atomic arrangements in Fe-based metallic glasses. Secondly, the Cu_2Mg type contains local atomic arrangements of icosahedron denoted by $12^{5.0}$ (coordination notation) and r (CS) whereas Fe_2P contains both trigonal prism capped with three half octahedron ($6^{5.0}3^{4.0}$, k) and ($12^{5.0}$, r), which are widely accepted to be the local atomic arrangements of metallic glasses. However, Co_2Si, $Mn_{12}Th$ and $CaCu_5$ types, which also contain $12^{5.0}$ in a part of their structures, are neglected in the present analysis because they are not the Laves phase. On the other hand, $MgZn_2$ is substituted for Cu_2Mg in the analysis owing to the facts that $MgZn_2$ is identical with Cu_2Mg in terms of CN and coordination in Table 1 and that the plots of $MgZn_2$ are covered by those of Cu_2Mg in the L-M-S diagram.

The ternary BMGs analyzed in the present study are summarized in Table 2 with sequential numbers and their references. The BMGs are categorized into L-, M- and S-types according to the relative atomic radius of the main constituent in each alloy [12]. Here, it is noted that the S-type is more

Table 2. Ternary BMGs used for the analysis, which are categorized into L(Large)-, M(interMediate)- and S(Small)- types according to the relative atomic size of the main constituent of each alloy, and are numbered sequentially from 1 to 22 with their reference numbers. The chemical formula of each BMG is written as $L_aM_bS_c$ (a+b+c = 100). The S-type is also widely defined as Transition Metal-type, since they forms BMGs with transition metals only.

L-type BMGs	M-type BMGs	S-type (Transition Metal-type) BMGs
1 ,$Zr_{60}Al_{15}Ni_{25}$ [17]	10 ,$Y_6Fe_{72}B_{22}$ [24]	16 ,$Zr_{30}Ti_{10}Cu_{60}$ [30]
2 ,$La_{55}Al_{25}Ni_{20}$ [18]	11 ,$Y_{10}Mg_{70}Cu_{20}$ [25]	17 ,$Sn_{6.9}Nb_{33.6}Ni_{59.5}$ [31]
3 ,$La_{50}Al_{25}Ni_{25}$ [18]	12 ,$Tb_{10}Mg_{65}Cu_{25}$ [26]	18 ,$Zr_{40}Ti_{10}Cu_{50}$ [32]
4 ,$Pd_{40}Ni_{40}P_{20}$ [19]	13 ,$Gd_{10}Mg_{65}Cu_{25}$ [27]	19 ,$Zr_{45}Ag_5Cu_{50}$ [32]
5 ,$Ca_{70}Mg_{20}Cu_{10}$ [20]	14 ,$Y_{10}Mg_{65}Cu_{25}$ [28]	20 ,$Zr_{45}Ag_{10}Cu_{45}$ [32]
6 ,$Ca_{60}Mg_{25}Ni_{15}$ [21]	15 ,$La_{20}Mg_{50}Ni_{30}$ [29]	21 ,$Zr_{50}Ag_5Cu_{45}$ [32]
7 ,$Ca_{65}Mg_{15}Zn_{20}$ [22]		22 ,$Zr_{47.5}Ag_{10}Cu_{42.5}$ [32]
8 ,$Ca_{60}Mg_{20}Zn_{20}$ [23]		
9 ,$Ca_{57}Mg_{19}Cu_{24}$ [20]		

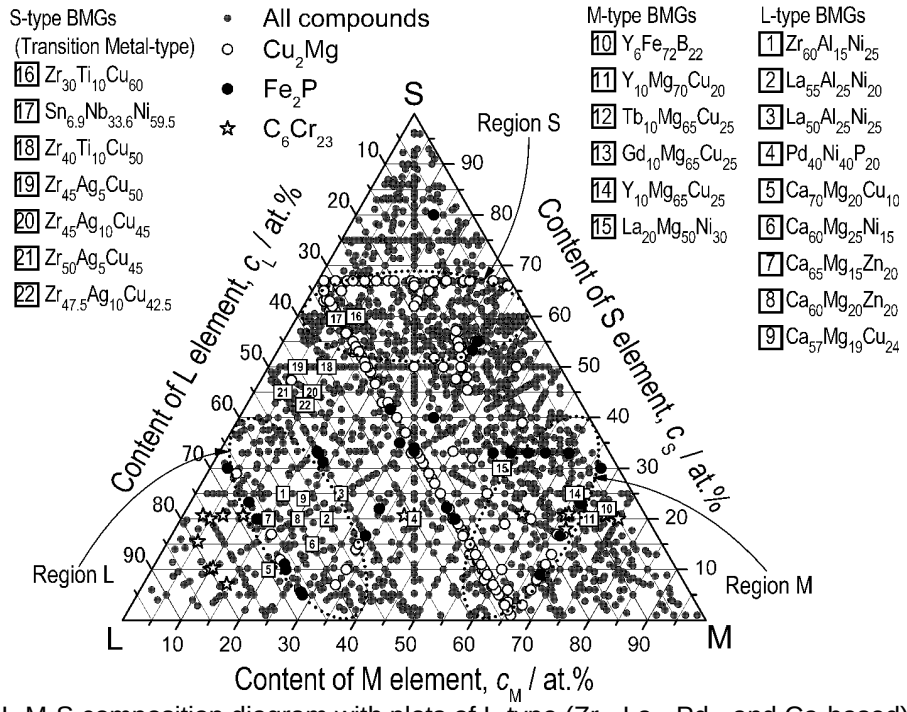

Fig. 1. The L-M-S composition diagram with plots of L-type (Zr-, La-, Pd-, and Ca-based), M-type (Fe- and Mg-based), and S-type (transition metal base) ternary BMGs, together with ternary compounds containing Cu_2Mg, Fe_2P and C_6Cr_{23} types. The sequential numbers from 1 to 22 with square are from Table 2. The ellipsoids drawn with dotted line at c_L, c_M and c_S of about 0.6 (Regions L, M, and S) are guide for eyes. The plots of 12 ,$Tb_{10}Mg_{65}Cu_{25}$ [26] and 13 ,$Gd_{10}Mg_{65}Cu_{25}$ [27] are substituted for the plot of 14 ,$Y_{10}Mg_{65}Cu_{25}$ [28] in the diagram.

widely defined as Transition Metal-type, since S-type BMGs consists of constituents belonging to transition metals only.

3. RESULTS AND DISCUSSION

Fig. 1 shows the L-M-S diagram with plots of 16873 ternary compounds containing Cu_2Mg, Fe_2P and

C_6Cr_{23} types and three types of ternary BMGs listed in Table 2. Fig. 1 reveals that the numbers of plots of all compounds are the highest in the Region S, and smallest in the Region L. Thus, the ternary compounds are readily formed in S-rich corner of the diagram. The Cu_2Mg type compounds are mainly plotted along the three composition regions of (1) c_L = 33.3 at.%, (2) c_S = 66.7 at.% and (3) c_M = 66.7 at.% and c_S < 20 at.% where the L- and M-types of BMGs are scarcely plotted. On the contrary, $Zr_{30}Ti_{10}Cu_{60}$ and $Sn_{6.9}Nb_{33.6}Ni_{59.5}$ belonging to S-type BMGs are plotted as part of the plots of Cu_2Mg type compounds at c_L = 33.3 at.% and the Region S as well. However, other S-type BMGs with sequential numbers from 18 to 22 are out of the plots of Cu_2Mg type compounds and Region S. This shift in the position of the plots of S-type BMGs takes place owing to the increase in glass-forming ability (GFA) [12] accompanied by the shift in main constituent with the smallest atomic size (Cu: in $Zr_{30}Ti_{10}Cu_{60}$) to the largest atomic size (Zr: in $Zr_{50}Ag_5Cu_{45}$ and $Zr_{47.5}Ag_{10}Cu_{42.5}$). Here, it is again noted that $Zr_{30}Ti_{10}Cu_{60}$, $Zr_{50}Ag_5Cu_{45}$ and $Zr_{47.5}Ag_{10}Cu_{42.5}$ are defined as S-type BMGs according to its wide definition that S-type BMGs consists of constituents belonging to transition metals only. As a whole, S-type BMGs are plotted at S-L side with c_M ~ 10 at.% of the L-M-S diagram, which is supported by the fact that atomic size difference is greater in S-L side than in S-M side at the S-corner.

The M-type BMGs are plotted near the edge of the Region M, in particular, in the M-S side at around $L_{10}M_{70}S_{20}$ where the ternary compounds are frequently found than the other side (L-M side) of the Region M. This is mainly due to the fact that the some of the Fe_2P and C_6Cr_{23} type compounds are plotted at around $L_{10}M_{70}S_{20}$ and that M-type BMGs presumably are producible at compositions by avoiding Laves phase with high melting temperature, which is located at M_2L in the L-M-S diagram.

Among the L-type BMGs, the plot of $Pd_{40}Ni_{40}P_{20}$ is isolated from the other plots of L-type BMGs in Fig. 1. However, $Pd_{40}Ni_{40}P_{20}$ shows similarity with the other L-type BMGs and the M-type BMGs with respect to the point that they are plotted at composition regions around c_S = 20 at.%. Another similarity between L- and M-type BMGs are seen in the plots of Fe_2P and C_6Cr_{23} type compounds that these compounds are plotted at the L-corner and the M-corner as well. This indicates the possibility of Fe_2P and C_6Cr_{23} types to influence the formation of L-type BMGs. The La-, Zr and Ca-based ternary BMGs are plotted at compositions around $L_{60}M_{20}S_{20}$ inside the Region L wherein the ternary compounds infrequently tend to be plotted than the other Regions. In addition, advantage of these L-type BMGs to be plotted at composition regions, which are regarded as anti-Laves compositions [5] to Cu_2Mg type compounds (Laves phase), is presumably the reason for the high GFA of the La-, Zr and Ca-based BMGs.

4. CONCLUSIONS

The formation of ternary bulk metallic glasses (BMGs) have been analyzed with the L-M-S diagram arranged by the order of the relative atomic radius of the constituent elements denoted by large, intermediate and small, and with the crystallographic data on ternary compounds. The L-M-S diagram with plots of ternary compounds reveals that ternary compounds in S-rich side of the diagram tend to form frequently than those in the other sides. The Fe_2P and C_6Cr_{23} type compounds directly affect the formation of Mg- and Fe-based BMGs and also influence that of La-, Zr- and Ca-based BMGs. The high glass-forming ability of La-, Zr- and Ca-based ternary BMGs is achieved due to their composition regions around $L_{60}M_{20}S_{20}$ in the L-M-S diagram where ternary compounds appear infrequently and anti-Laves relationship to Cu_2Mg type compounds holds in ternary systems.

REFERENCES

[1] W. Klement, R.H. Willens and P. Duwez // *Nature* **187** (1960) 869.
[2] A. Inoue // *Acta Mater.* **48** (2000) 279.
[3] W. Hume-Rothery and E. Anderson // *Phil. Mag.* **5** (1960) 383.
[4] H.S. Chen // *Acta Metall.* **24** (1976) 153.
[5] R.St. Amand and B.C. Giessen // *Scripta Metall.* **12** (1978) 1021.
[6] J.D. Bernal // *Nature* **185** (1960) 68.
[7] P.H. Gaskell // *J. Non-Cryst. Solids* **32** (1979) 207.
[8] C. Park, M. Saito, Y. Waseda, N. Nishiyama and A. Inoue // *Mater. Trans. JIM* **40** (1999) 491.
[9] M. Imafuku, S. Sato, H. Koshiba, E. Matubara and A. Inoue // *Mater. Trans., JIM* **41** (2000) 1526.
[10] J.L. Uriarte, A.R. Yavari, S. Surinach, P. Rizzi, G. Heunen, M. Baricco, M.D. Haro and A. Kvick // *J. Mag. Mag. Mater.* **254** (2003) 532.

[11] D.B. Miracle // *Nature Mater.* **3** (2004) 697.
[12] A. Takeuchi and A. Inoue // *Mater. Trans.* **46** (2005) 2817.
[13] *Metal databook, 4th edition* (Japan Institute of Metals, Maruzen), p. 4, In Japanese.
[14] *Smithells Metals Reference Book, 8th edition*, ed. by W.F. Gale and T.C. Totemeir (Elsevier Inc., The Netherlands, 2004), Chapter 4.
[15] *Structure of Binary Compounds*, ed. by F.R. de Boer and D.G. Pettifor (Elsevier Science Publishers B.V., 1989, North Holland, 1989).
[16] *Handbook of Ternary Alloy Phase Diagrams*, ed. by P. Villars, A. Prince and H. Okamoto (ASM International, USA, 1995).
[17] A. Inoue, T. Zhang and T. Masumoto // *Mater. Trans. JIM* **31** (1990) 177.
[18] A. Inoue, T. Zhang and T. Masumoto // *Mater. Trans. JIM* **30** (1989) 965.
[19] H.W. Kui, A.L. Greer and D. Turnbull // *Appl. Phys. Lett.* **45** (1984) 615.
[20] K. Amiya and A. Inoue // *Mater. Trans.* **43** (2002) 81.
[21] E.S. Park and D.H. Kim // *Appl. Phys. Lett.* **86** (2005) 201912.
[22] E.S. Park and D.H. Kim // *J. Mater. Res.* **19** (2004) 685.
[23] K. Amiya and A. Inoue // *Mater. Trans.* **43** (2002) 2578.
[24] C.Y. Lin, H.Y. Tien and T. S. Chin // *Appl. Phys. Lett.* **86** (2005) 162501.
[25] A. Inoue, T. Nakamura, N. Nishiyama and T. Masumoto // *Mater. Trans. JIM* **33** (1992) 937.
[26] X.K. Xi, D.Q. Zhao, M.X. Pan and W.H. Wang // *J. Non-Cryst. Solids* **344** (2004) 189.
[27] H. Men, W.T. Kim and D.H. Kim // *J. Non-Cryst. Solids* **337** (2004) 29.
[28] A. Inoue, A. Kato, T. Zhang, S.G. Kim and T. Masumoto // *Mater. Trans. JIM* **32** (1991) 609.
[29] A. Inoue, M. Kohinata, A.P. Tsai and T. Masumoto // *Mater. Trans. JIM* **30** (1989) 378.
[30] A. Inoue, W. Zhang, T. Zhang and K. Kurosaka // *Mater. Trans.* **42** (2001) 1149.
[31] H. Choi-Yim, D.H. Xu and W.L. Johnson // *Appl. Phys. Lett.* **82** (2003) 1030.
[32] W. Zhang and A. Inoue // *J. Mater. Res.* **21** (2006) 234.